OCC Performance Optimization Based on the Variation of Camera and LED Parameters

Kazi Afra Nawer¹, Mostafa Zaman Chowdhury¹, and Yeong Min Jang²

¹Department of Electrical and Electronic Engineering, Khulna University of Engineering & Technology, Khulna 9203, Bangladesh

²Department of Electronics Engineering, Kookmin University, Seoul 02707, Korea

Email: afra.khl@nwu.ac.bd, mzaman@eee.kuet.ac.bd, yjang@kookmin.ac.kr

Abstract—Optical camera communication (OCC) is an optimistic substitute for the current radio frequency (RF) based communication. It is a promising branch of optical wireless communication (OWC) that involves camera image sensor to capture optical signal from LED transmitter rather than typical photodetector. This paper offers a comprehensive analysis on various parameters of the camera and the light source, focusing on the optimization of the performance of an OCC system. Accordingly, the impact of size and shape of the light source and focal length of the camera lens is investigated to amplify the communication range of OCC. The investigation finds that, certain shapes of light source aid to achieve optimal distance in OCC. Moreover, this paper also analyzed the effect of multiple camera parameters on the signal to noise ratio (SNR) of the OCC system. The camera parameters include lens f-number and camera exposure time. The analysis finds that longer camera exposure time and certain value of f-number lead to better SNR performance. In this investigation LED radiation pattern, camera noise sources and environmental condition are considered.

Keywords— Camera exposure time, image sensor (IS), lens focal length, lens f-number, light emitting diode (LED), optical camera communication (OCC), signal to noise ratio (SNR).

I. INTRODUCTION

Intelligent transportation system (ITS) is emerging as one of the promising fields of interest due to its widely recognized applications in developing countries. In ITS, vehicles trade information with other vehicles and highway traffic control infrastructures through wireless technologies [1]. As a congruent substitute for the present radio frequency (RF) wireless technologies, the implementation of optical wireless communication (OWC) in vehicle to vehicle (V2V) and vehicle to infrastructure (V2I) communications can be very functional due to its cost-free massive spectrum, as well as the rapid development of highway traffics and infrastructures [2]. In recent years, optical camera communication (OCC) has gathered remarkable attention as a promising subsystem of OWC. OCC is basically a visible light communication (VLC) with image sensor (IS) based optical receivers (i.e. cameras) that has an array of photodiodes (PDs), termed as pixels, whereas varieties of lasers or light emitting diodes (LEDs) are utilized as optical transmitters [3]. One lucrative feature of IS is that, at the same time it can detect several light sources within its field of view (FOV). The IEEE 802.15.7m amendment focused on the development of OCC system [4].

Nowadays, the extensive uses of smartphones with integrated complementary metal-oxide-semiconductor (CMOS) cameras, modern vehicles with front and rare cameras and LED-based lights, street lights, dashboards and

smart devices for road surveillance has revealed a remarkable dimension in the field of OCC system [5], [6]. Exposing the cameras to the LED transmitters can serve multi-purpose of imaging, video streaming, as well as receiving transmitted data. Currently available commercial LEDs provide high energy efficiency, long lifespan, minimal power consumption, high switching speed, modulation capability, and they are quite affordable. The widespread implementation of these LEDs offers bright lighting and information transmission simultaneously [7], [8].

In OCC, visible light does not require any license unlike RF, the system is resilient to electromagnetic interference from other RF communication, and the system provide higher spectral efficiency [9]. The line of sight (LOS) properties and the spatial separability feature of the camera limit the interference from other light sources. Moreover, as compared to other OWC technologies, there is very little impact of interference on OCC [10]. However, OCC system faces several challenges, including: (i) cameras cannot spot LEDs blinking at high frequency; (ii) the low frame rates particularly in global shutter-based cameras cause visible flickering; (iii) conventional cameras offer lower sampling rates, causing lower data rates (a few kbps) as compared to PD-based receivers; and (iv) synchronizing the modulation frequency of the LED and the shutter speed of the camera. Implementation of CMOS based rolling-shutter cameras and proper modulation methods may overcome flickering and increased the data rates [2], [5]. Over the past few years, various research works are done to enhance the performance of OCC.

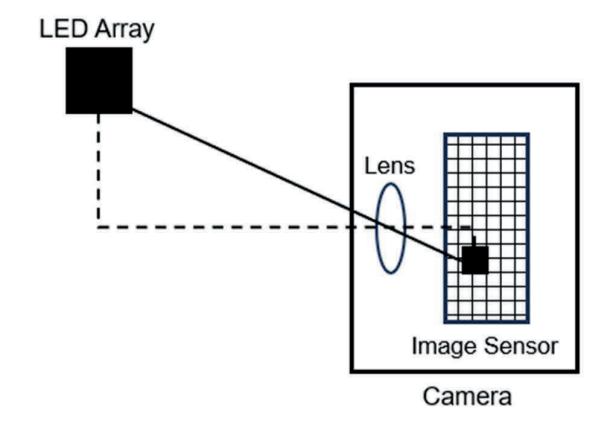


Fig. 1. A simple OCC system.

The system performance of OCC depends upon the camera parameters as well as the LED characteristics. Shape and size of LED array have significant impact on the performance of OCC system, which is discussed in this paper. Considering the OCC model illustrated in Fig. 1, the rest of the paper investigates the impact of some important camera parameters on the system performance of OCC. Section II provides the system model, the performance analysis is shown in Section III, and finally Section IV draws the conclusion of the work.

II. SYSTEM MODELING

A. Model Setup

This model considers an OCC system with LOS configuration as illustrated in Fig. 1, where the LED array and the camera are used as optical transmitter (Tx) and optical receiver (Rx) respectively.

B. Focal Length and F-Number

The focal length of a camera determines the amount of a scene captured by the camera. The projected image area on the camera focal panel depends on the lens focal length, f_o and the pixel edge length of the image sensor, ρ and is given by [11],

$$A_F = \frac{A_{LED} f_o^2}{d^2} \tag{1}$$

where A_{LED} denotes the effective area of LED array exposed to illumination and d is the distance between LED array and camera. A_F can also be expressed in terms of pixels by simply being divided by ρ^2 .

Lens f-number or f-stop or the focal ratio indicates the light gathering ability of the lens. A smaller value of f-number denotes a broader aperture, enabling more light to pass through the lens. It is the ratio of the lens focal length and the lens aperture diameter and is given by [12],

$$F_N = \frac{f_0}{dia} \tag{2}$$

where dia is the aperture diameter of the lens.

C. LED Array Shape

The initial step of captured image processing is localizing the LED array position in the image. The detection algorithms are designed considering several characteristics of the LED array. A detection algorithm is proposed in [13]. LED arrays are well-defined and compact in shape. In order to determine the maximum possible communication distance in LOS configuration, it is important to figure out the smallest possible image size projected on the focal panel of the camera. To make the communication successful the smallest image projected on the camera focal panel must entirely cover at least one pixel on the focal panel. A 3×3 array of focal panel is considered for this calculation. For circular LED array, only the projected image with a diameter of 2.3ρ completely covers a pixel on the focal panel as shown in Fig. 2(c). The images with smaller size than that do not fully cover a pixel on the focal panel as illustrated in Figs. 2(a) and 2(b). Figs. 3(a), 3(b), and 3(c) demonstrate that, in case of square LED array, the projected image with edge length 2ρ fully covers a pixel on the focal panel, but the images with smaller area do not

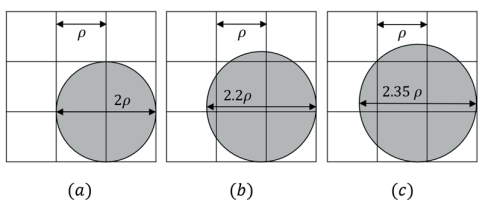


Fig. 2. Illustration of the projected image of circular LED array on the focal panel of the camera with, (a) diameter 2ρ , (b) diameter 2.2ρ , and (c) diameter 2.35ρ .

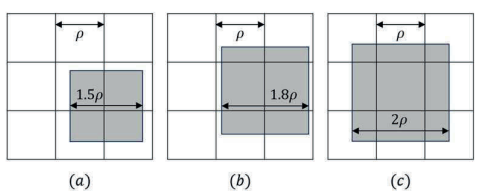


Fig. 3. Illustration of the projected image of square LED array on the focal panel of the camera with, (a) edge length 1.5ρ , (b) edge length 1.8ρ , and (c) edge length 2ρ .

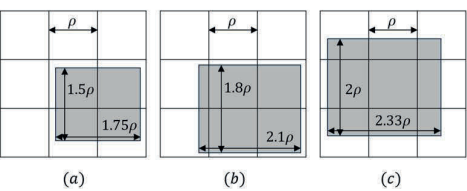


Fig. 4. Illustration of the projected image of rectangular LED array (7:6 edge ratio) on the focal panel of the camera with, (a) dimension $1.5\rho \times 1.75\rho$, (b) dimension $1.8\rho \times 2.1\rho$, and (c) dimension $2\rho \times 2.33\rho$.

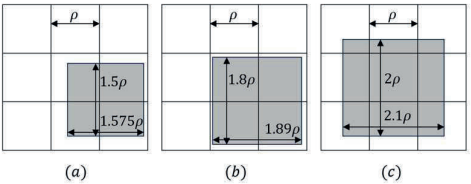


Fig. 5. Illustration of the projected image of rectangular LED array (21:20 edge ratio) on the focal panel of the camera with, (a) dimension $1.5\rho \times 1.575\rho$, (b) dimension $1.8\rho \times 1.89\rho$, and (c) dimension $2\rho \times 2.1\rho$.

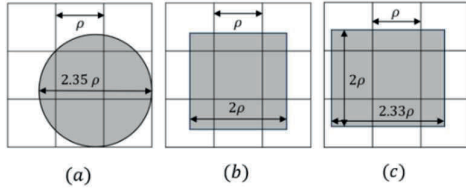


Fig. 6. Illustration of smallest possible image projected on the focal panel of the camera for (a) circular LED array, (b) square LED array, and (c) rectangular LED array.

completely cover a pixel on the focal panel. For rectangular LED array with edge ratio of 7:6, the projected image with dimension $2\rho \times 2.33\rho$ entirely covers a pixel on the focal panel, but the images with smaller area do not cover a pixel completely as demonstrated in Figs. 4(a), 4(b), and 4(c). Figs. 5(a), 5(b), and 5(c) illustrate that, for rectangular LED array with edge ratio of 21:20, the projected image on the focal panel with dimension $2\rho \times 2.1\rho$ entirely covers a pixel on the focal panel. Any image that is smaller in size does not cover a pixel completely. It is clearly visible from Fig. 6. that, with the change in shape of the LED array, the smallest possible image size on the focal panel varies.

D. Lambertian Illumination Model

Here, a Lambertian radiation pattern is considered for the light source. The Lambertian radiant intensity is presented by [14],

$$R_0(\varphi_{ir}) = \frac{(1 + m_L) P_T \cos^{m_L}(\varphi_{ir})}{2\pi}$$
 (3)

where φ_{ir} denotes the LED irradiance angle and P_T represents the optical power transmitted. m_L is the order of Lambertian emission model, which is originated from half power radiation angle, $\varphi_{\frac{1}{2}}$ and is expressed as [14],

$$m_L = -\frac{\ln 2}{\ln \left(\cos \varphi_1\right)} \tag{4}$$

E. Optical Power Transmitted

For OCC in outdoor environment, the weather conditions have impact on the transmitted signal, thereby affecting the system performance. Both attenuation and dispersion are present in the channel. Beer-Lambert law is implemented to characterize the attenuation. Then, for LOS arrangement of OCC, the received power in each pixel of the IS is given by [15],

$$P_{R} = \begin{cases} \frac{\pi T_{l} I(\varphi_{ir})}{4 F_{N}^{2} A_{LED}} \cdot \frac{A_{P} \cos(\varphi_{in})}{LER} \cdot e^{(-d\gamma)}, & A_{F} > A_{P} \\ \frac{I(\varphi_{ir}) A_{l} T_{l} \cos(\varphi_{in})}{d^{2} LER} \cdot e^{(-d\gamma)}, & A_{F} \leq A_{P} \end{cases}$$
(5)

where T_l denotes the camera lens transmittance, A_l is the area of the lens, φ_{in} is the incident angle, LER stands for luminous efficiency of radiation, F_N denotes the lens f-number, γ represents extinction coefficient, and $I(\varphi_{ir})$ denotes the beam luminous intensity (in cd). The area of a pixel of the IS is given by [5],

$$A_P = \frac{k_{FF} A_I}{N \times M} \tag{6}$$

where A_I is the IS area, k_{FF} indicates the pixel fill factor, and N, M are the dimensions of the IS in pixel.

F. SNR

As a measure of the OCC system performance the signal to noise ratio (SNR) is considered in this study. Noise parameters, including photo response non-uniformity (PRNU), source follower noise, photon shot noise, dark current shot noise, and sense node reset noise are taken into account on the basis of the IS model proposed in [16]. The source follower noise has a Gaussian distribution and incorporates flicker noise, thermal noise (or Johnson noise), and random telegraph noise (RTN). The dark current noise is resulted from the thermally generated electron discharge, which is explained by Poisson process. The dark current is given by [16],

$$i_{dc} = qA_P I_{FOM} T^{3/2} ex p\left(\frac{-E_{gap}}{2 k_B T}\right)$$
 (7)

where q represents the charge of electron, T is the temperature in K, I_{FOM} denotes the dark current figure-of-merit at 300K in nA/cm^2 , E_{gap} is the band gap energy of Si in eV, and k_B denotes the Boltzmann's constant. Change in material characteristics of substrate during the fabrication process of IS

TABLE I. IMPORTANT PARAMETER FOR SYSTEM MODELING

Parameter	Value
Transmitted optical power	1.5 W
Incidence angle	0°
Irradiance angle	0°
Half power radiation angle	60°
Lens transmittance	0.75
Number of pixels	1080×1920
Pixel fill factor	0.3 A/W
Pixel responsivity	0.5
Extinction coefficient	0.69 dB/Km
Luminous efficiency of radiation	250.3 lm/W
Reset noise standard deviation	70 e-
Source follower standard deviation	6 e-
Photo response non-uniformity standard deviation	1 %
Band gap energy of Si	1.1108 eV
Operating temperature	300 K
Dark current figure-of-merit	1 nA/cm ²

is the principal source of PRNU, which can be modeled implementing a Gaussian distribution. Then, the SNR is given by,

$$SNR = 10 \log_{10} \left(\frac{(i_{pc} t_e)^2}{q (i_{pc} + i_{dc}) t_e + q^2 (\sigma_{Reset}^2 + \sigma_{SF}^2) + (\sigma_{PNRU} i_{pc} t_e)^2} \right)$$
(8)

where σ_{SF}^2 and σ_{Reset}^2 are source follower noise variance and reset noise variances respectively, σ_{PNRU} denotes the standard deviation of the PRNU, and t_e denotes the IS exposure time. The pixel photocurrent is given by [5],

$$i_{nc} = R.P_R \tag{9}$$

where *R* denotes CMOS pixel responsivity.

G. Channel Capacity

The channel capacity of OCC system may be expressed in terms of maximum achievable data rates (bits/sec) and varies with the modulation approach employed in the system [17],

$$C_{capacity} = F_R W_{SB} \log_2(M) \tag{10}$$

where F_R denotes camera frame rate in fps, W_{SB} denotes spatial bandwidth, which can be defined as the number of information carrying pixels per camera image frame. M is the modulation order, e.g. M = 2 for BPSK, M = 4 for 4-QAM.

III. PERFORMANCE ANALYSIS

This section represents the simulation outcomes to evaluate the proposed OCC system performance using different values of some important camera and LED parameters. A camera is placed at a distance d from the LED array as illustrated in the proposed model in Fig. 1. All other important system parameters used in the simulation are included in Table I.

Figs. 7, 8 and 9 illustrate that, the size of projected image on the focal panel amplifies with increasing lens focal length. This simulation is performed for a communication distance of 200 m. Fig. 7 demonstrates that, greater value of focal length results in greater no. of pixels of the image. It is also found that, for a given focal length (say 26 mm), larger circular LED array provides greater no. of pixels of the projected image. Similarly, Figs. 8 and 9 illustrate the effects of LED array size and camera focal length on the no. of pixels of the projected

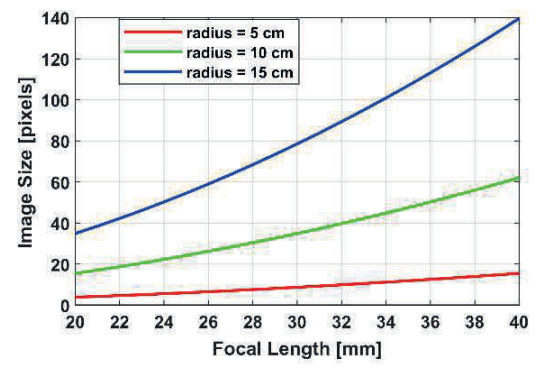


Fig. 7. Variation of image size against varying lens focal length for different size of circular LED array.

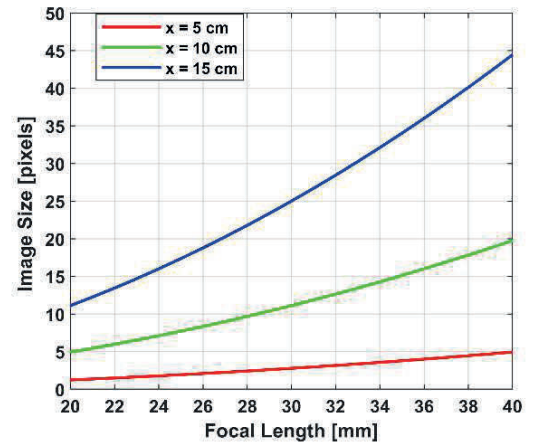


Fig. 8. Variation of image size against varying lens focal length for different size of square LED array.

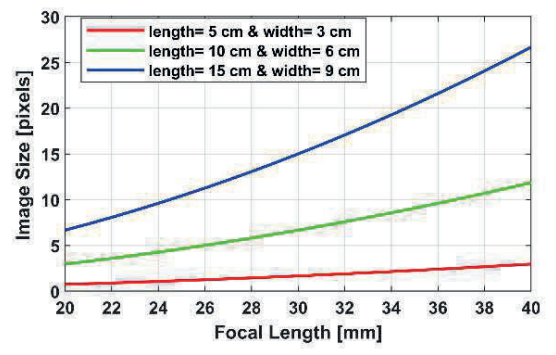


Fig. 9. Variation of image size against varying lens focal length for different size of rectangular LED array.

image for square LED array and rectangular LED array respectively. The impact of LED array size on communication range for circular LED array, square LED array, rectangular LED array with 7:6 edge ratio, and rectangular LED array with 21:20 edge ratio are observed in Figs. 10 to 13 respectively. It is found that, the increase in LED array size leads to communication range enhancement. Moreover, maximum range of communication is obtained from the greatest value of the camera focal length. Fig. 14 demonstrates the effect of LED array shape on communication distance. It indicates that, for a given size of LED array (say 100 cm²), square shape LED array provides greater communication range as compared to other shapes of LED array under similar condition. It also demonstrates that, circular shape LED array provides better

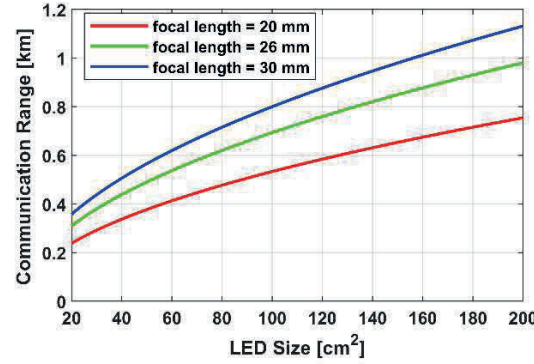


Fig. 10. Variation of communication range against varying LED array size for circular LED array and different lens focal length.

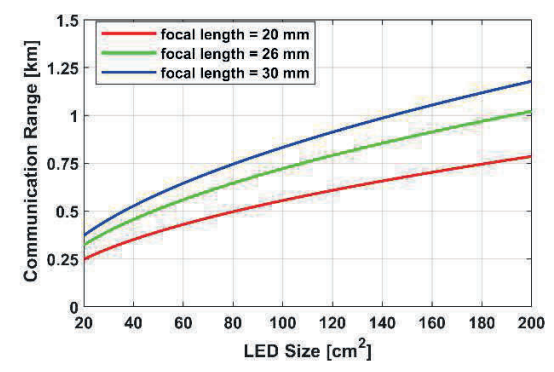


Fig. 11. Variation of communication range against varying LED array size for square LED array and different lens focal length.

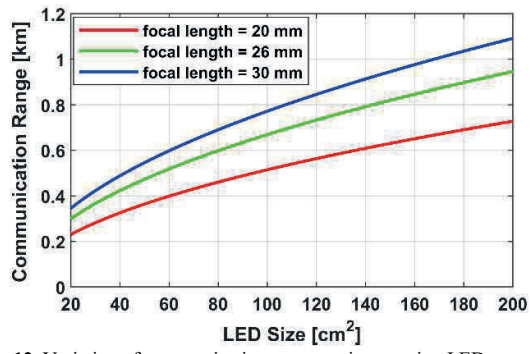


Fig. 12. Variation of communication range against varying LED array size for rectangular LED array (7:6 edge ratio) and different lens focal length.

performance than rectangular LED array with 7:6 edge ratio, but lower performance than rectangular LED array with 21:20 edge ratio. In this investigation, the size of the LED array is considered to be 100 cm². Figs. 15 to 18 focus on the effect of camera lens focal length on communication range for circular LED array, square LED array, rectangular LED array with 7:6 edge ratio, and rectangular LED array with 21:20 edge ratio respectively. It is observed that, for a given LED array area (say 80 cm²), greater value of lens focal length gives rise to the communication range. Also, it is visibly clear that, LED array with grater size leads to higher range of communication. So, it can be summarized that, lens focal length and LED array size both have significant impact on communication range.

Fig. 19 illustrates that, for a given value of lens focal length (say 26 mm), square shape LED array gives slightly longer communication range as compared to other shapes of LED array under similar environment. It is also visible that,

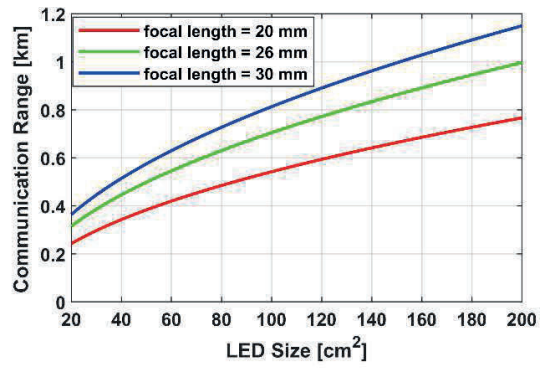


Fig. 13. Variation of communication range against varying LED array size for rectangular LED array (21:20 edge ratio) and different lens focal length.

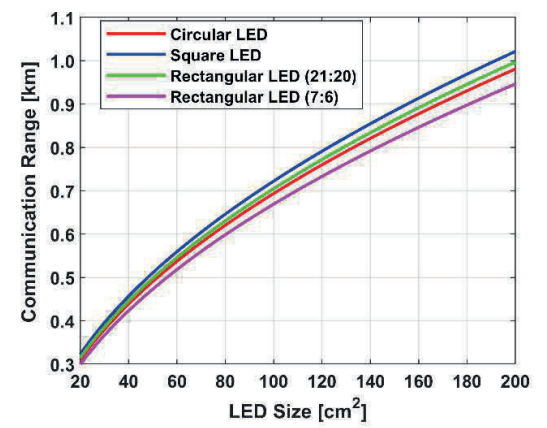


Fig. 14. Variation of communication range against varying size of LED array for different shape of LED array.

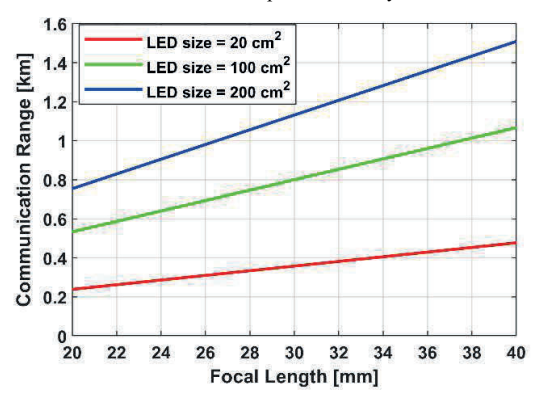


Fig. 15. Variation of communication range against varying lens focal length for circular LED array.

circular LED array gives better performance than rectangular LED array with 7:6 ratio, but poorer performance than rectangular LED array with 21:20 edge ratio under similar condition. In this analysis, the area of the LED array is assumed to be 100 cm². Fig. 20 demonstrates that, the value of SNR drops with increase in the distance between the LED array and the camera, particularly at a distance greater than 560 m. It also shows the effect of the lens f-number on SNR of the system. Recalling (2), it is known that lower value of f-number results in greater lens diameter. Hence, at a given communication distance (say 350m), greater lens size (i.e. lower f-number) provides greater value of SNR. A square shape LED array with an area of 400 cm² and the IS of 336

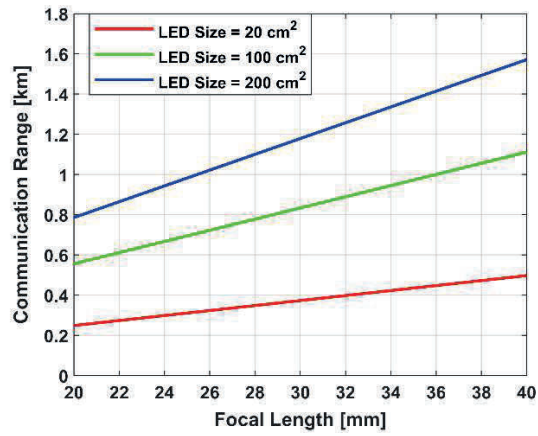


Fig. 16 Variation of communication range against varying lens focal length for square LED array.

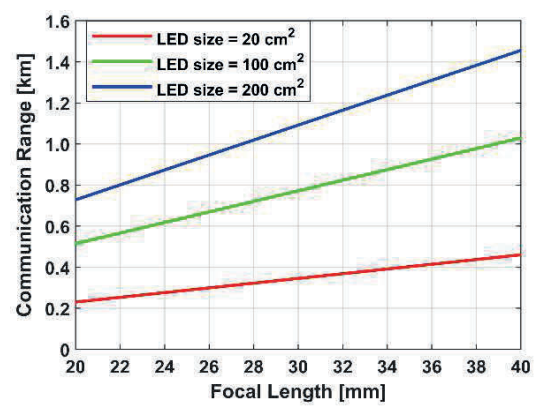


Fig. 17. Variation of communication range against varying lens focal length for rectangular LED array (7:6 edge ratio).

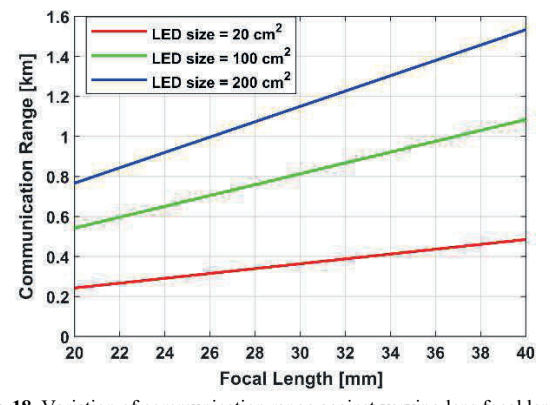


Fig. 18. Variation of communication range against varying lens focal length for rectangular LED array (21:20 edge ratio).

mm² area with a focal length of 26 mm are considered in this investigation. In this simulation all noise conditions are taken into account. The camera is exposed for data reception for 10 µs. The impact of camera exposure time on SNR is demonstrated in Fig. 21. Considering the lens focal length and the f-number to be 26 mm and 2.8 respectively, it is illustrated that, SNR value decreases with increasing distance and at a given distance (say 400 m) longer camera exposure time results in higher value of SNR. But longer exposure time may cause inter-symbol interference if the LED is blinking faster. It limits the camera frame rate. Recalling (10), this causes low data rate.

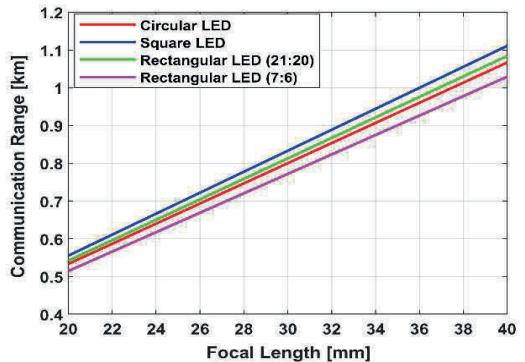


Fig. 19. Variation of communication range against varying lens focal length for different shape of LED array.

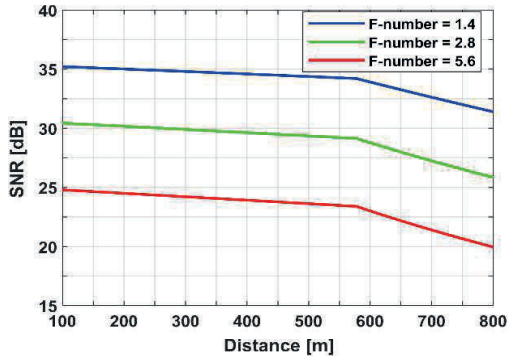


Fig. 20. Variation of SNR against communication distance for different camera f-number.

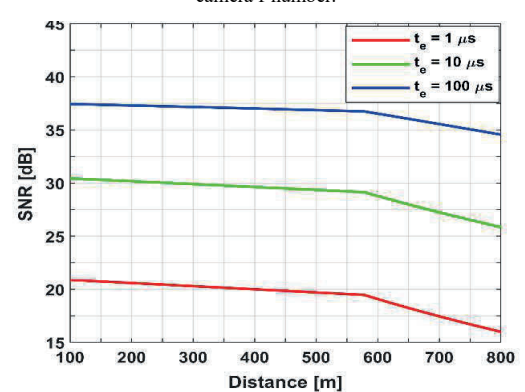


Fig. 21. Variation of SNR against communication distance for different camera exposure time.

IV. CONCLUSION

As an optimistic field of OWC system and a congruent complement to the existing RF technologies, OCC is playing a vital role in releasing burden on the currently available spectrum. In OCC, with only a minimal modification the easy-accessible cameras are utilized to capture data from conventional LEDs mounted on infrastructures, vehicles or simply hand-held mobile devices. In this study, an OCC model with LOS arrangement is proposed to investigate the effect of certain camera parameters including lens focal length, lens f-number, and camera exposure time on the performance of the OCC system. It is observed that, by increasing the camera lens focal length, we can improve the OCC system performance. This study paid a great deal of attention to the selection of size and shape of LED array. It is

seen that, certain shapes of LED array provide better and longer range of communication. Considering the noise parameters, this work also analyzed the behavior of SNR as a measure of OCC performance evaluation. This work proves that, shorter communication distance, longer camera exposure time and lens f-number of smaller value offer better SNR.

Acknowledgement: This work was supported by the National Research Foundation of Korea (NRF) Grant funded by Korean Government (MSIT) under Grant 2022R1A2C1007884.

REFERENCES

- M. Uysal, Z. Ghassemlooy, A. Bekkali, A. Kadri, and H. Menouar, "Visible light communication for vehicular networking: performance study of a V2V system using a measured headlamp beam pattern model," *IEEE Veh. Technol. Mag.*, vol. 10, no. 4, pp. 45–53, Dec. 2015.
- [2] M. Z. Chowdhury, M. T. Hossan, A. Islam, and Y. M. Jang, "A comparative survey of optical wireless technologies: Architectures and applications," *IEEE Access*, vol. 6, pp. 9819–10220, Jan. 2018.
- [3] H. Nguyen and Y. M. Jang, "Experimental demonstration of deep learning-based HS2PSK-OFDM scheme for optical camera communication," *ICT Express*, June 2025.
- [4] M. M. Rahman, M. S. Nazim, M. I. Joha, and Y. M. Jang, "Real-time implementation of OFDM modulation for an OCC system: UNet-based equalizer for signal denoising and BER optimization," *ICT Express*, vol. 11, no. 4, pp. 728-733, Aug. 2025.
- [5] N. M. Esfahani, A. Gholami, N. S. Kordavani, S. Zvanovec, and Z. Ghassemlooy, "The impact of camera parameters on the performance of V2V optical camera communications," 12th Int. Symposium on CSNDSP, Porto, Portugal, 2020, pp. 1-4.
- [6] K. Eöllős-Jarošíková et al., "Wearable shaped side-emitting fiber transmitters for optical camera communication," *Journal of Lightwave Technology*, vol. 43, no. 7, pp. 3183-3193, Apr. 2025.
- [7] D. Karunatilaka, F. Zafar, V. Kalavally, and R. Parthiban, "LED based indoor visible light communications: State of art," *IEEE Communications Surveys & Tutorials*, vol. 17, no. 3, pp. 1649-1678, thirdquarter 2015.
- [8] A. Liu, W. Shi, M. Safari, W. Liu, and J. Cao, "Design guidelines for optical camera communication systems: A tutorial," *IEEE Photonics J.l*, vol. 16, no. 4, pp. 1-25, Aug. 2024.
- [9] H. Herfandi et al., "Implementation of a multiple-transmitter RS-OFDM-based OCC system with advanced bytetrack for mobility environments," *IEEE Access*, vol. 13, pp. 119411-119426, 2025.
- [10] I. Takai et al., "Optical vehicle-to-vehicle communication system using LED transmitter and camera receiver," *IEEE Photonics J.*, vol. 6, no. 5, pp. 1-14, Oct. 2014.
- [11] M. K. Hasan, M. Z. Chowdhury, M. Shahjalal, V. T. Nguyen, and Y. M. Jang, "Performance Analysis and Improvement of Optical Camera Communication," *Appl. Sci.*, vol. 8, no. 12, p. 2527, Dec. 2018.
- [12] F. Lei and L. K. Dang, "Measurement of the numerical aperture and fnumber of a lens system by using a phase grating," *Appl. Opt.*, vol. 32, pp. 5689–5691, 1993.
- [13] T. Do and M. Yoo, "A simple LED panel dection algoritum for Optical Camera Communication systems," *International Conference on Information and Communication Technology Convergence (ICTC)*, Jeju, Korea (South), 2019, pp. 747-749.
- [14] W. Viriyasitavat, S. H. Yu, and H. M. Tsai, "Channel model for visible light communications using off-the-shelf scooter taillight," *IEEE Veh. Netw. Conf. VNC*, Boston, MA, USA, 2013, pp. 170-173.
- [15] M. S. Z. Sarker et al., "Design and implementation of a CMOS light pulse receiver cell array for spatial optical communications," *Sensors*, vol. 11, no. 2, pp. 2056–2076, Feb. 2011.
- [16] W. Huang and Z. Xu, "Characteristics and Performance of Image Sensor Communication," *IEEE Photonics J.*, vol. 9, no. 2, pp. 1-19, Apr. 2017.
- [17] A. Islam, L. Musavian, and N. Thomos, "Performance analysis of vehicular optical camera communications: Roadmap to uRLLC," *IEEE Global Communications Conference*, Waikoloa, USA, 2019, pp. 1-6.